Journal of Photochemistry and Photobiology A: Chemistry 207 (2009) 79–85

Contents lists available at ScienceDirect

Journal of Photochemistry and Photobiology A: Chemistry

journal homepage: www.elsevier.com/locate/jphotochem

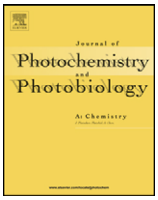

Phosphorescence quenching of a platinum acetylide polymer by transition metal ions

Katsu Ogawa, Fengqi Guo, Kirk S. Schanze*

Department of Chemistry, University of Florida, P.O. Box 117200, Gainesville, FL 32611-7200, USA

ARTICLE INFO

Article history:
Available online 3 May 2009

Keywords:
Phosphorescence quenching
Amplified quenching effect
Platinum acetylide
Bipyridine
Transition metal ions

ABSTRACT

A platinum acetylide-based polymer (p-Pt_2BPyPh) that contains 2,2′-bipyridine units in the polymer backbone has been synthesized. A model complex (Pt_2BPyPh_2) has also been prepared that features the same structure as a single polymer repeat unit. The polymer and model complex exhibit moderately efficient and long-lived phosphorescence emission from a triplet excited state. The effect of addition of six different transition metal ions (Fe^{3+}, Co^{2+}, Zn^{2+}, Ni^{2+}, Cu^{2+} and Pd^{2+}) on the absorption and phosphorescence spectra of p-Pt_2BPyPh and Pt_2BPyPh was examined. The results show that in every case, the metal ions bind to the bipyridine unit in the polymer (model) backbone, and metal ion binding induces a red-shift in the near-UV absorption band. Phosphorescence spectroscopy shows that for all of the metals (with the exception of Zn^{2+}), metal ion binding is accompanied by phosphorescence quenching. For some of the metal ions (Cu^{2+} and Ni^{2+}) quenching of the polymer is considerably more efficient than in the model, an observation consistent with an "amplified quenching effect" that is analogous to that observed for quenching of fluorescent conjugated polymers. A semi-quantitative analysis of the absorption and phosphorescence data provide a model consistent with the notion that triplet exciton hopping along the polymer chain is rapid compared to the triplet lifetime, and that the overall quenching efficiency for the different metal ions is controlled by the intrinsic rate of triplet quenching within the metal ion–bipyridine complex.

1. Introduction

In the past few decades, π-conjugated polymers (CPs) and oligomers have received significant research interest due to their unique electronic and optical properties. Potential applications for these materials include organic light emitting diodes [1,2], organic photovoltaic devices [3–5], and chemical sensors [6,7]. The sensory application is based on the discovery that CPs exhibit "amplified luminescence quenching" by charge neutral or ionic quenchers that are present at very low concentration [8–12]. This effect is due to delocalization and rapid diffusion of singlet excitons along the polymer backbone. Such properties suggest that CPs have the potential to be more sensitive chemical sensors than systems based on small molecular luminophores.

Due to environmental and biological concerns, selective and sensitive sensors capable of detecting trace concentrations of metal ions are needed [13]. Conjugated polymers featuring bipyridine or terpyridine units on the side chains have been shown to exhibit amplified fluorescence quenching effects when the metal complexing units bind to transition metal ions [14,15]. In another approach to metal ion sensing, 2,2′-bipyridine units were incorporated into backbone of a poly(phenylene vinylene)-based CP. The absorption and emission properties of the material were altered significantly upon coordination of a variety of metal ions to the bipyridine units. It was shown that such change in photophysical behavior is due to (1) the extension of the conjugation length of the polymer backbone induced by coordination of metal ions to 2,2′-bipyridine units; and (2) the change in the HOMO-LUMO gap due to the interaction of the a positively charged metal ion with the bipyridine moiety [16].

Although fluorescent chemical sensors are well known, only a few examples of transition metal ion sensors based on phosphorescence quenching can be found in the literature [17–19]. Platinum acetylide-type CPs and oligomers have gained much attention due to their phosphorescent properties with potentials for a variety of applications [20–23]. The previous work demonstrated that triplet excitons are confined within two or three repeat units of a Pt-acetylide conjugated backbone [24]. Although triplet excitons are much less delocalized in comparison to singlet excitons in the same π-conjugated system, their long lifetimes and potential for intra- or inter-chain triplet exciton migration lead to potential for sensitive chemosensing materials. In addition, the study of the interaction of platinum acetylide polymers with quencher ions can provide considerable insight concerning the extent of triplet

---

* Corresponding author. Tel.: +1 352 392 9133; fax: +1 352 846 0296.
E-mail addresses: mogawa@chem.ufl.edu (K. Ogawa), fqguo@zzu.edu.cn (F. Guo), kschanze@chem.ufl.edu (K.S. Schanze).

1010-6030/$ – see front matter © 2009 Elsevier B.V. All rights reserved.
doi:10.1016/j.jphotochem.2009.04.013

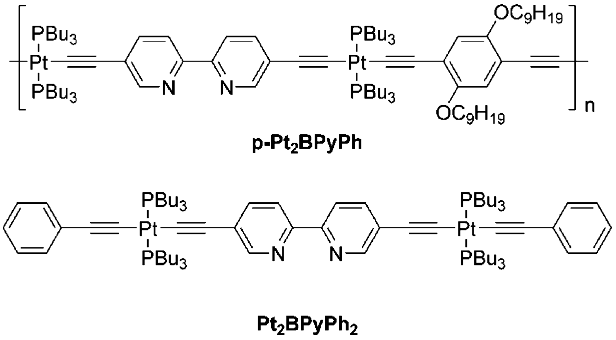

Scheme 1. Structures of p-Pt$_2$BPyPh and Pt$_2$BPyPh$_2$.

exciton delocalization and its ability to migrate along the polymer backbone.

This report describes the synthesis and characterization of a novel platinum(II)-acetylide-based conjugated polymer that features 2,2′-bipyridine units incorporated into the backbone as transition metal ion binding sites (p-Pt$_2$BPyPh, Scheme 1). This polymer exhibits strong phosphorescence at ambient temperature, and the luminescence can be quenched by addition of a variety of transition metal ions. In order to provide a model system to explore the ability of the polymer to amplify the quenching effect, we also synthesized and studied the quenching response of the model complex Pt$_2$BPyPh$_2$ (Scheme 1) which is essentially a single repeat unit of p-Pt$_2$BPyPh.

2. Results and discussion

2.1. Synthesis

The polymer p-Pt$_2$BPyPh was synthesized by the multi-step reaction scheme shown in Scheme 2. Dichlorobis(tributylphosphine) platinum [25], 2,2′-bipyridine hydrobromide (**2**) [26], 5,5′-dibromo-2,2′-bipyridine (**3**) [26], and 5,5′-diethynyl-2,2′-bipyridine (**4**) [27] were synthesized according to the literature procedure. Polymerization was effected via a CuI-catalyzed Hagihara coupling protocol [28]. Initially, attempts were made to incorporate the monomer 2,5-bisbutyloxy-1,4-diethynylbenzene in the polymer backbone. However, the resulting polymer was insoluble in all solvents tested, presumably because the butyl groups were not sufficiently long to induce solubility of the material. Thus, 2,5-bisnonyloxy-1,4-diethynylbenzene moiety was chosen as an alternative monomer, and the resulting polymer, p-Pt$_2$BPyPh was quite soluble in solvents such as THF and CHCl$_3$. The model complex and polymer were characterized by NMR spectroscopy. In addition, the molecular weight of p-Pt$_2$BPyPh was determined by gel permeation chromatography affording a number averaged molecular weight of M_n = 7160 (polydispersity index = 2.0). The observed M_n value suggests that the average degree of polymerization (number of repeat units in an average chain) is in the range of 4–5.

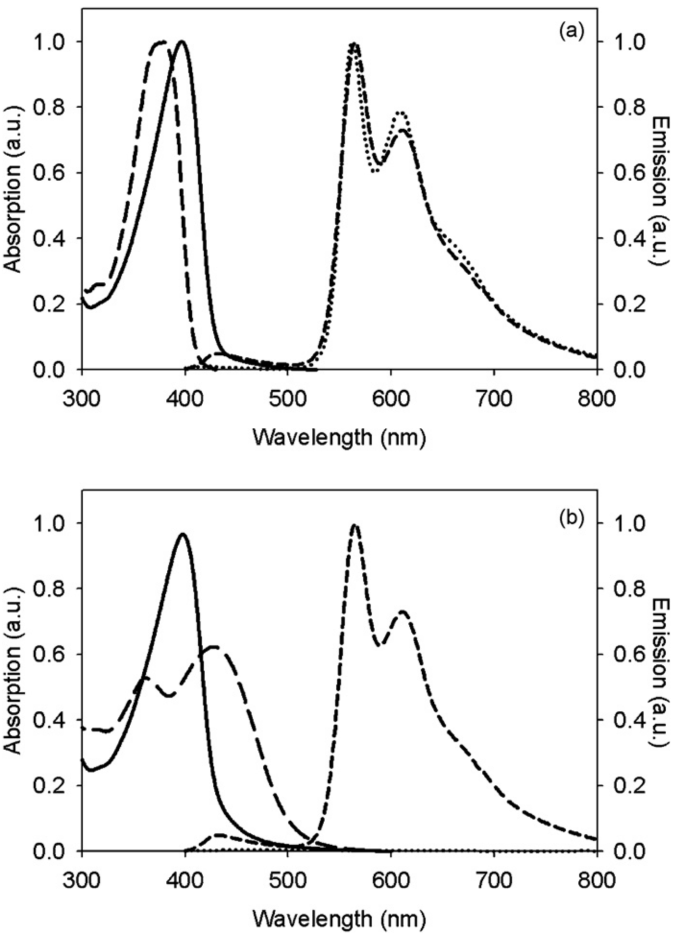

Fig. 1. (a) Absorption spectra of p-Pt$_2$BPyPh (——) and Pt$_2$BPyPh$_2$ (— — —) and emission spectra of p-Pt$_2$BPyPh (– – –) and Pt$_2$BPyPh$_2$ (·····) in THF-CH$_3$OH (10:1) solution. (b) Absorption spectra of p-Pt$_2$BPyPh in THF-CH$_3$OH (10:1) solution in neutral (——) and acidic (— — —) conditions, and emission spectra in neutral (– – –) and acidic (·····) conditions.

2.2. Photophysical properties

As seen in Fig. 1a, the model complex Pt$_2$BPyPh$_2$ exhibits a narrow absorption band with λ_{max} = 379 nm. The polymer p-Pt$_2$BPyPh has a similar absorption band, but the band maximum is slightly red-shifted to λ_{max} = 396 nm, suggesting a slight increase

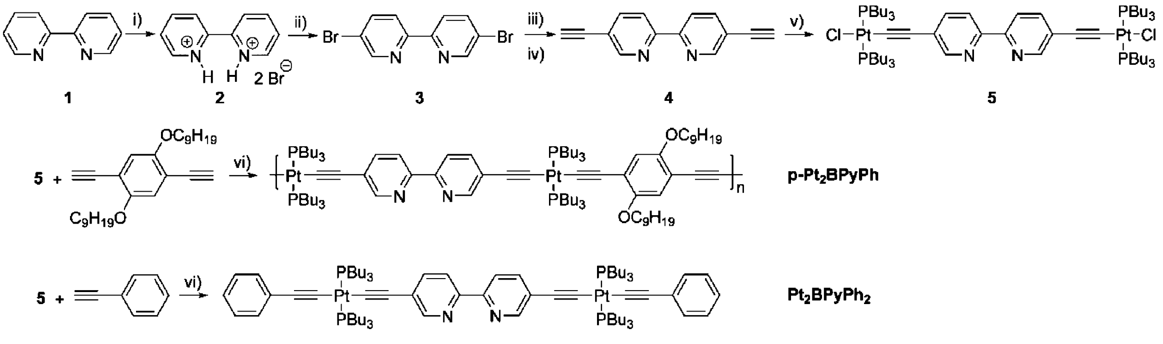

i) CH$_3$COBr, CH$_3$OH; ii) Br$_2$, 180°C; iii) Me$_3$SiCCH, Pd(PPh$_3$)$_2$Cl$_2$, CuI, ^{i}Pr$_2$NH; iv) NaOH(aq); v) Pt(PBu$_3$)$_2$Cl$_2$, piperidine; vi) CuI

Scheme 2. Synthesis of p-Pt$_2$BPyPh and Pt$_2$BPyPh$_2$.

Table 1
Photophysical properties of Pt_2BPyPh_2 and p-Pt_2BPyPh.

Compound	λ_{abs}/nm (ε/cm^{-1} M^{-1})	λ_{em}/nm	Φ_{em}	τ_{T1}/μs
Pt_2BPyPh_2	379 (90,500)	562, 610	0.12	85
p-Pt_2BPyPh	396 (109,600)	565, 610	0.065	58

in the degree of π-conjugation in the polymer. The photoluminescence spectra of the complexes are dominated by a broad band with λ_{max} = 565 nm which is Stokes shifted considerably from the absorption band. In deoxygenated solution the lifetime of the emission is 85 μs and 58 μs for Pt_2BPyPh_2 and p-Pt_2BPyPh, respectively, consistent with assignment of the emission to phosphorescence from the triplet excited state. The interesting feature is that the phosphorescence spectra of Pt_2BPyPh_2 and p-Pt_2BPyPh are nearly coincident, a feature that suggests that in both systems the triplet exciton is concentrated on a single repeat unit consisting of a Pt–C≡C-bpy–C≡C–Pt unit. This observation is consistent with other reports in the literature which suggest that the spatial extent of triplet exciton is relatively small in π-conjugated systems [23,29,30].

Virtually no fluorescence can be observed from the model complex Pt_2BPyPh_2, and only weak fluorescence can be observed from p-Pt_2BPyPh at λ_{max} = 430 nm. This observation suggests that intersystem crossing in both systems is very efficient, likely induced by strong spin–orbit coupling due to the heavy atom effect of the platinum centers (although quantum yields for intersystem crossing were not determined in the present study, intersystem crossing yields in structurally similar platinum acetylide oligomers and polymers are typically >90%) [23]. The phosphorescence quantum efficiency was determined to be 0.12 and 0.065 for Pt_2BPyPh_2 and p-Pt_2BPyPh, respectively. The lower phosphorescence efficiency for the polymer arises due to a more efficient non-radiative decay, most likely the result of quenching due to end-groups and inter-chain interactions in polymer aggregates. Note that the ratio of the phosphorescence lifetimes for the model and polymer is approximately the same as the ratio of the phosphorescence quantum efficiencies; this fact indicates that the radiative rate is approximately the same in the two systems. The photophysical properties of the materials are summarized in Table 1.

The effect of addition of acid (H^+) on the spectroscopic properties of Pt_2BPyPh_2 and p-Pt_2BPyPh was explored by addition of HCl to THF:CH_3OH solutions of the materials. As shown in Fig. 1b, addition of HCl to a solution of p-Pt_2BPyPh results in a splitting of the absorption into two bands, with the most intense transition shifting to longer wavelength, λ_{max} = 427 nm. This red-shift indicates that protonation of the bipyridine unit induces a reduction in the HOMO-LUMO gap. This reduction arises because the positive charge associated with protonation effectively stabilizes the unfilled levels more than the filled levels, resulting in a decrease in the HOMO-LUMO gap. Similar effects have been observed in other bipyridine-containing π-conjugated oligomers and polymers, and the effect has also been explored theoretically [31]. Addition of acid also causes complete quenching of polymer's phosphorescence emission. Apparently the protonated bipyridine unit is able to effectively quench the triplet exciton, most likely via a charge transfer mechanism. Importantly, the absorption and emission spectral changes are reversible, as neutralization of the acidified solution by addition of hydroxide ion resulted in recovery of the original absorption and emission spectra.

2.3. Effect of transition metal ions on absorption and phosphorescence

The changes in the photophysical properties of Pt_2BPyPh_2 and p-Pt_2BPyPh induced by addition of Fe^{3+}, Co^{2+}, Ni^{2+}, Cu^{2+}, Zn^{2+}, and Pd^{2+} ions were studied for solutions of the materials in THF/CH_3OH mixed solvent. In general, binding of metal ions to the bipyridine units of Pt_2BPyPh_2 and p-Pt_2BPyPh induces significant changes in both the absorption and emission of the materials. Fig. 2 illustrates the effects that addition of Cu^{2+} has on the absorption and emission of p-Pt_2BPyPh; these effects are similar to those observed concomitant with addition of the other metal ions (with some exceptions, see below). As seen in Fig. 2a, increased concentration of Cu^{2+} induces a formation of new red-shifted band at λ ~ 440 nm; note that this band is similar to that seen coincident with addition of H^+ to the polymer solution (vide supra). The absorption band shift, accompanied by an isosbestic point suggests that binding of the metal ion increases the conjugation length of the polymer backbone, effectively lowering the HOMO-LUMO gap. In particular, upon coordination to a metal ion, the bipyridine unit is forced into a planar conformation, which increases the conjugation length. The changes seen upon binding of metals to p-Pt_2BPyPh are very similar to the results reported by Wang and Wasielewski for interaction of metals with a bipyridine substituted poly(phenylene vinylene) [16]. Addition of most metal ions to both Pt_2BPyPh_2 and p-Pt_2BPyPh induces the formation of the new red-shifted absorption band ions; however, addition of Co^{2+} and Zn^{2+} did not induce similar changes. This observation can be explained by the very low stability constants of these two metal ions for binding with bipyridine unit (vide infra).

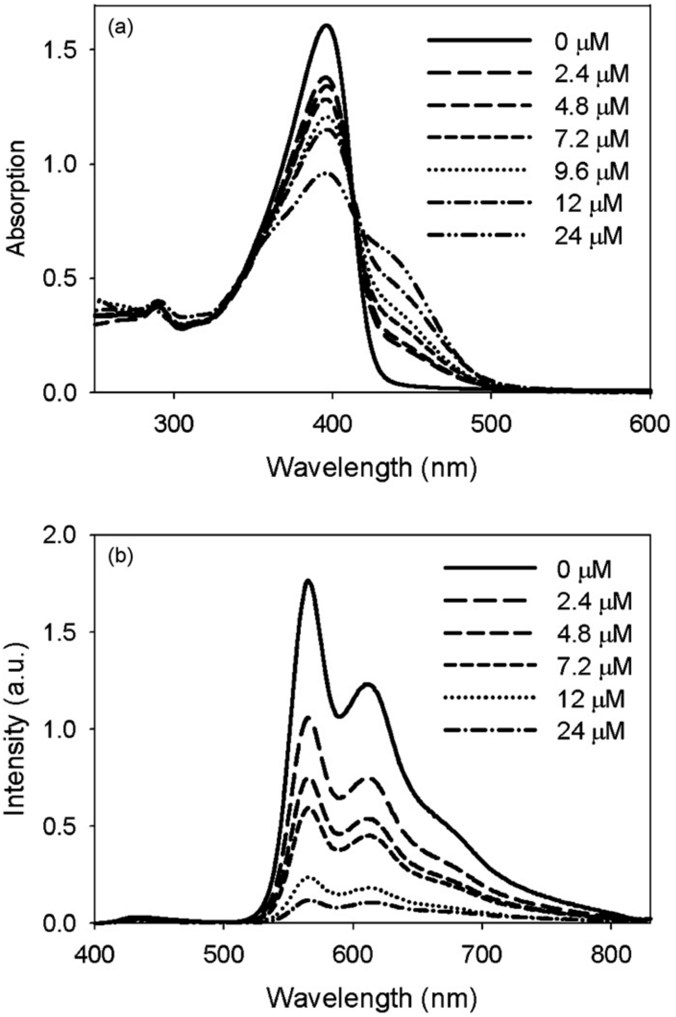

Fig. 2. (a) Absorption and (b) emission spectra of p-Pt_2BPyPh in THF/CH_3OH (10:1) solution (12.0 μM) in the presence of Cu^{2+} ion.

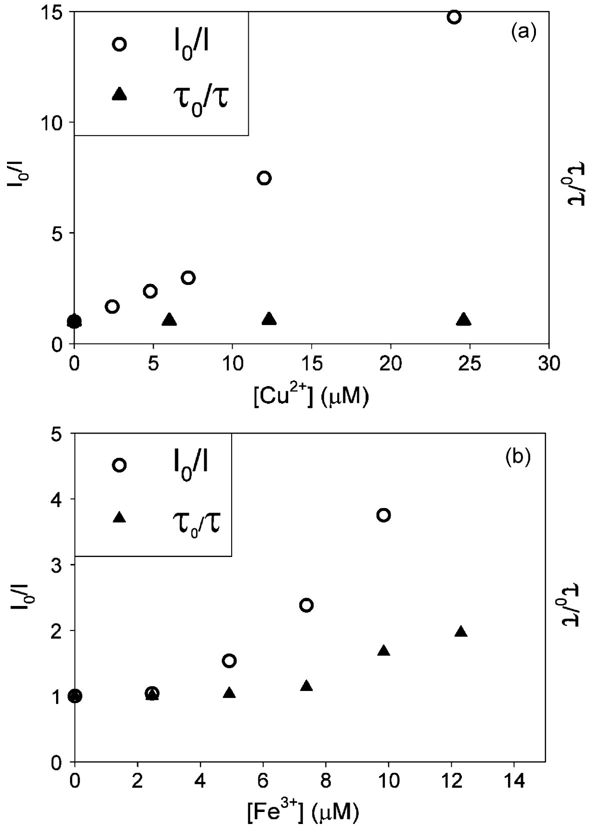

Fig. 3. Stern–Volmer plots of p-Pt_2BPyPh emission intensity and lifetime quenched by metal ions in THF/CH_3OH (10:1) solution at room temperature. (a) Cu^{2+} and (b) Fe^{3+}. The concentration of the p-Pt_2BPyPh corresponding to the repeat unit was 12.0 μM.

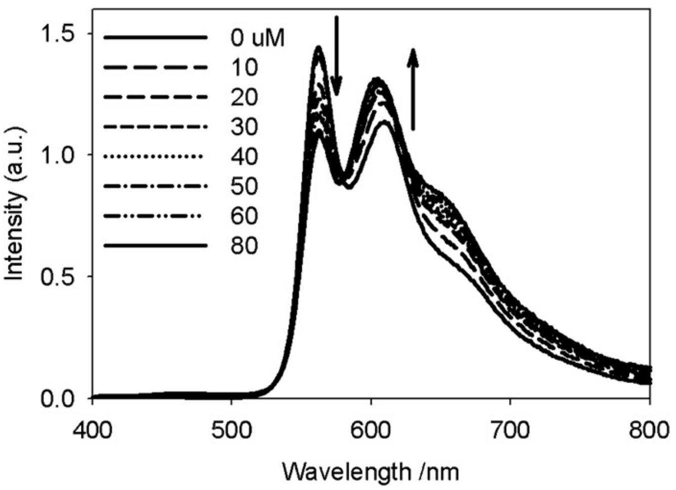

Fig. 4. Emission spectra of Pt_2BPyPh_2 in THF/CH_3OH (10:1) solution (12.0 μM) in the presence of Zn^{2+} ion.

Addition of metal ions to Pt_2BPyPh_2 and p-Pt_2BPyPh not only causes changes in the absorption spectra, but also leads to quenching of the phosphorescence, even at very low concentration of added metal ion. Depending on the metal, the quenching mechanism likely involves either (photoinduced) charge transfer or energy transfer to metal-centered excited states. Stern–Volmer (SV) phosphorescence intensity quenching studies were carried out for both Pt_2BPyPh_2 and p-Pt_2BPyPh. In general, the SV plots are curved upward at higher metal ion concentration, and an example plot is seen in Fig. 3 which shows the SV plots for Cu^{2+} and Fe^{3+}. Table 2 contains the SV quenching constants (K_{SV}) which were computed from the linear region of the SV plots at low metal ion concentrations. For most of the metal ions, the K_{SV} values are larger for p-Pt_2BPyPh_2 than for Pt_2BPyPh, indicating that there is some amplification of the quenching in the polymer. A more detailed analysis of the relative quenching efficiencies is provided below.

Phosphorescence lifetime studies were also carried out, and in general it was found that for the same quencher concentration the lifetimes are quenched less than the emission intensity. An example SV lifetime plot for Cu^{2+} is also shown in Fig. 3a. For this ion the lifetime changes little over the full range of concentration studied. This result indicates that the phosphorescence quenching occurs by a static mechanism, i.e., the dynamics of quenching within a metal ion polymer complex are rapid compared to the natural triplet lifetime. A second example lifetime plot is shown in Fig. 3b for Fe^{3+}. Interestingly, in this case there is some lifetime quenching; however, the lifetime is quenched less than the total emission intensity. This observation suggests that for Fe^{3+} quenching occurs by a mixed mode mechanism, with contributions from static and dynamic modes. The reason for the different behavior of Cu^{2+} and Fe^{3+} will be discussed below where a kinetic model for the quenching is developed.

Although addition of Fe^{3+}, Co^{2+}, Ni^{2+}, Cu^{2+}, and Pd^{2+} to Pt_2BPyPh_2 and p-Pt_2BPyPh induces phosphorescence quenching, addition of Zn^{2+} to the model complex is an exception, as in this case the phosphorescence spectrum only undergoes spectral shifts. Specifically, as shown in Fig. 4, addition of Zn^{2+} to a solution of Pt_2BPyPh_2 causes a decrease in the emission band at 562 nm and an increase in the band at 610 nm as well as a new band around 660 nm. The presence of isoemissive point suggests that the new band is due to the emission from the metal-coordinated species. This observation is consistent with the fact that Zn^{2+} is a closed shell ion and therefore does not induce phosphorescence quenching (the Zn^{2+}–Pt_2BPyPh_2 is emissive).

2.4. Stability constants for metal–bipyridine complexation

A key objective of this work was to attempt to determine the number of repeat units in the polymer that are effectively quenched in the polymer–metal ion complexes. This result would provide insight concerning the effective number of repeat units in the polymer that are sampled by the triplet exciton during its lifetime.

Table 2

Stern–Volmer constants, fractions of bpy unit bound to Pt_2BPyPh_2, corresponding stability constants, fractions of quenched emission of p-Pt_2BPyPh at equivalent concentration (12 μM of each species) of metal ion and the coordination sites, and the effective number polymer repeat unit quenched.

	K_{SV}/M^{-1} Pt_2BPyPh_2	K_{SV}/M^{-1} p-Pt_2BPyPh_2	Stability constant (log *K*)	Fraction of PRUs complexed	Fraction of quenched polymer emission	PRUs quenched per bound metal[a]
Fe^{3+}	1.4×10^5	1.5×10^5	5.38	0.55	0.88	1.6
Co^{2+}	8.0×10^3	1.3×10^4	3.67	0.047	0.047	1.0
Ni^{2+}	1.1×10^4	1.8×10^5	4.02	0.094	0.69	7.4
Cu^{2+}	2.8×10^4	2.8×10^5	4.29	0.15	0.87	5.6
Pd^{2+}	4.1×10^4	1.9×10^5	4.64	0.26	0.82	3.1

[a] Calculated by dividing column 6 by column 5.

In order to address this problem, we sought to use the emission quenching data for binding of the metal ions to the model complex to determine the stability constants for binding of the metals to the bipyridine unit. Then, by assuming that the stability constants are the same for binding of the metals to the model and polymer, we can use the stability constants to compute the fraction of bipyridine units in the polymer that are bound at any particular metal ion concentration.

Thus, a literature procedure was followed in order to estimate the stability for binding of the metal ions to Pt_2BPyPh_2 at ambient temperature [32]. The fraction of ligand bound to metal ion ($[ML]/C_L$) can be obtained by the following equation:

$$\frac{ML}{C_L} = \frac{I_0 - I}{I_0}$$

where $[ML]$ is the concentration of metal–ligand complex (the metal ion–Pt_2BPyPh_2 complex), C_L is the total concentration of the ligand (Pt_2BPyPh), I_0 is the emission intensity in the absence of added metal ion, and I is the emission intensity in the presence of metal ion. (This expression assumes that the phosphorescence is completely quenched in the metal ion–Pt_2BPyPh complex.) For each metal ion, the fraction of coordinated Pt_2BPyPh that is complexed was obtained by comparing the phosphorescence intensity before (I_0) and after (I) the addition of one equivalent ($c = 12\ \mu M$) of metal ion quencher. Metal ion–bipyridine stability constants (formation constants) K at ambient temperature can be obtained from

$$K = \frac{[ML]}{[M][L]}$$

where $[M]$ and $[L]$ are the concentrations of the unbound metal and the free ligand (Pt_2BPyPh_2), respectively. The stability constants are listed in the fourth column of Table 2, and they range from $>10^5\ M^{-1}$ for Cu^{2+} and Fe^{3+} to $\sim 5 \times 10^3\ M^{-1}$ for Co^{2+}.

2.5. Analysis of polymer quenching: triplet exciton diffusion

Assuming that the stability constant is the same for the polymer and model complex, it is possible to compute the fraction of bipyridine polymer repeat units (PRUs) in the polymer that are complexed when the polymer and metal ion concentration are $12\ \mu M$. This calculation was carried out, and the results are listed in the fifth column of Table 2 (fraction of PRUs complexed). Here it can be seen that at the relatively low polymer and metal ion concentrations used in the quenching studies metal ion binding is incomplete, even though one equivalent of metal ion is present per bipyridine PRU in the polymer. With this in mind, it is interesting to compare the fraction of PRUs complexed with the quenching efficiency in the polymer. The significant feature is that for some metals (e.g., Cu^{2+} and Ni^{2+}) quenching is nearly complete, even though only a relatively small fraction of PRUs contain metal ion quenchers (10–15%). For the other metals quenching is much less complete, even though in some cases (e.g., Fe^{3+}) a substantial fraction of PRUs are complexed.

A different perspective of this effect is shown in Fig. 5, which compares the fraction of phosphorescence quenched, $(I_0 - I)/I_0$, for the polymer vs. the fraction of PRUs that are complexed for titration with the five different metal ions. Here again it is seen that for Cu^{2+} and Ni^{2+}, quenching is nearly complete quenching when only 20% of the PRUs are complexed; however, for the other metals quenching is only complete when a greater fraction of PRUs are occupied by metal ions.

At this point we turn to consider the implications of the correlations of quenching efficiency and metal ion binding to the bipyridine PRUs in $p\text{-}Pt_2BPyPh_2$. We posit that the ratio of the quenching efficiency in the polymer to the number of PRUs bound by metal ions (Table 2, column 6 divided by column 5) reflects the effective number of repeat units in the polymer that are quenched per bound metal ion. This number is computed for each of the metal ion quenchers, and the results are listed in the last column of Table 2. Interestingly, for Cu^{2+} and Ni^{2+}, which are the most efficient quenchers of $p\text{-}Pt_2BPyPh_2$, the number of PRUs quenched per bound metal ion is approximately equal to the degree of polymerization. This correspondence suggests that for these metals, binding of a single metal ion to a polymer chain leads to complete quenching of any triplet excitons that are produced on the chain. By contrast, for Co^{2+} and Fe^{2+}, the quenching is much less efficient; complete quenching is achieved only when nearly all of the bipyridine PRUs are complexed. (See Fig. 5 and note that in order to achieve a fraction of bound PRUs approaching unity an excess of metal ion needs to be added to the solution.)

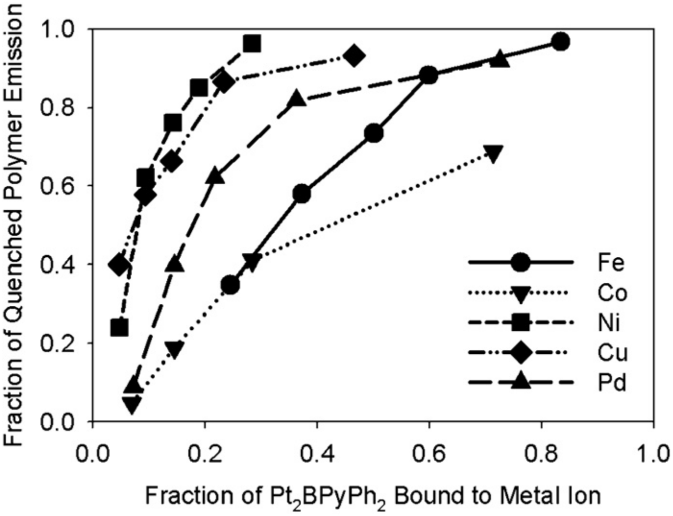

Fig. 5. Correlation between emission quenching and fraction of bipyridine units complexed for $p\text{-}Pt_2BPyPh$. Fraction of units complexed was computed using the association constants listed in Table 2.

A qualitative kinetic model that explains the different behavior of the metal ion quenchers is provided in Scheme 3. In this model we define two rate processes: k_{th} which is the rate for triplet exciton hopping between PRUs on the polymer, and k_{tq} which is the rate for triplet quenching when the triplet exciton is on a PRU that is complexed to a metal ion quencher (e.g., Cu^{2+}, Fe^{3+}, etc.). In this model there are two limiting cases: (1) triplet hopping is slower than triplet quenching ($k_{th} < k_{tq}$); (2) triplet hopping is faster than triplet quenching ($k_{th} > k_{tq}$). This model can be used to explain the different behavior of the various quencher ions. In particular, for Cu^{2+} and Ni^{2+}, we suggest that limiting case 1 holds. In this case the efficiency of phosphorescence quenching is limited only by the dynamics of triplet hopping along the polymer chain, and every time that a triplet exciton arrives at a bound PRU it is quenched. Furthermore, in this kinetic regime, if triplet hopping along the chain is fast compared to the triplet lifetime, then quenching will be very efficient even when only a single PRU is complexed to a metal ion quencher. Note also that the observation that quenching is static for Cu^{2+} (Fig. 3a) is consistent with limiting case 1. In a sep-

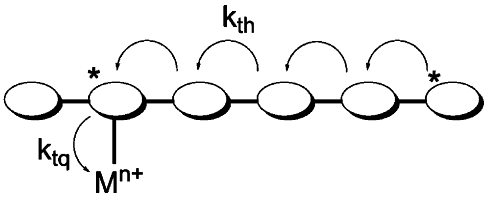

Scheme 3. A kinetic model of quenching mechanism.

arate unpublished study we have demonstrated that in a platinum acetylide oligomer that is structurally similar to p-Pt_2BPyPh_2 the rate of triplet hopping (k_{th}) is greater than 10^{10} s^{-1}. Given that the natural triplet lifetime in p-Pt_2BPyPh_2 is in the μs time domain, then it is reasonable to expect that quenching will be very efficient for Cu^{2+} and Ni^{2+} if both k_{tq} and k_{th} are >10^9 s^{-1}, which seem very reasonable possibilities.

Perhaps more interesting is the behavior of the less efficient quencher ions, Fe^{3+} and Co^{2+}. In these systems, we suggest that kinetic case 2 holds; in particular, while triplet exciton hopping along the chain is fast, the intrinsic rate of quenching (k_{tq}) is relatively slow and consequently, the triplet exciton is not quenched every time that it arrives onto a metal ion complexed PRU. This mechanism could be termed the “drive by mechanism”, where the triplet exciton is able to migrate past (i.e., drive by) a quencher bound PRU many times before it becomes quenched. In this case because the intrinsic quenching rate is relatively low, other processes can compete with triplet exciton quenching such as metal ion association or disassociation and diffusion of the metal ion to a polymer chain. Because of these competing processes, dynamic quenching is expected, and note that consistent with this expectation for Fe^{3+} mixed mode quenching is observed (Fig. 3b).

The reason that the intrinsic quenching rate (k_{tq}) is considerably less for Fe^{3+} and Co^{2+} compared to Ni^{2+} and Cu^{2+} is unclear. Previous studies of diffusional quenching of organic triplet states by metal ions indicate that quenching is close to diffusion controlled for these ions [33], so the reason for the different behavior in the present case is not clear at this time.

3. Summary and conclusion

A novel platinum acetylide-based conjugated polymer that contains 2,2′-bipyridine moieties in every polymer repeat unit has been synthesized, along with a model complex that features a single bipyridine binding unit. The polymer and model complex display moderately efficient phosphorescence that emanates from the triplet excited state. Absorption and phosphorescence studies carried out in the presence of a series of six transition metal ions provide evidence that the metal ions complex to the bipyridine moiety, and in most cases metal ion–bipyridine complexation is accompanied by quenching of the phosphorescence. For Cu^{2+} and Ni^{2+}, the phosphorescence quenching is much more efficient in the polymer than in the model complex, indicating that there is effective amplified quenching in the polymer. For several other metal ions (e.g., Co^{2+} and Fe^{3+}) comparable quenching efficiency is seen for the polymer and model complex. A semi-quantitative analysis which takes into account the association constants for the metal ions to the bipyridine unit suggests that the difference in quenching efficiency for the metal ions arises in part due to variation of the stability constants, but mainly due to the difference in intrinsic quenching efficiency in the metal ion–bipyridine complex. The results are consistent with a model in which diffusion of the triplet exciton along the platinum acetylide chain is rapid compared to its lifetime (k_{th} > 10^9 s^{-1}).

4. Experimental section

4.1. General synthetic procedures and source of starting materials

2,2′-Bipyridine, $Ni(OAc)_2$, $Pd(OAc)_2$, and $FeCl_3$ were purchased from Aldrich Chemical Company. $Co(OAc)_2$, $Zn(OAc)_2$, $Cu(OAc)_2$, spectroscopy grade THF and methanol were purchased from Fisher Scientific Company. Unless otherwise noted, chemicals were used without further purification. Dichlorobis(tributylphosphine) platinum [25], 2,2′-bipyridine hydrobromide (**2**) [26], 5,5′-dibromo-2,2′-bipyridine (**3**) [26], and 5,5′-diethynyl-2,2′-bipyridine (**4**) [27] were synthesized according to the literature procedure.

4.2. Characterization methods

Unless otherwise noted, ^1H, ^{13}C, and ^{31}P NMR spectra were recorded on a Varian Mercury 300 MHz spectrometer and chemical shifts are reported in ppm relative to the peak for TMS. Steady state UV–visible absorption spectra were obtained on a Cary 100 spectrometer. Steady state photoluminescence spectra were collected on a SPEX Fluorolog-2 spectrophotometer. Time resolved emission spectra and lifetimes were collected with samples contained in a 1 cm path length cell on an apparatus described elsewhere [34]. The phosphorescence quantum yields are measured using $Ru(bpy)_3{}^{2+}$ ($\Phi_f = 0.055$) [35] as an actinometer. A mixture of THF and methanol (10:1) was used as the solvent in all the photophysical measurements. All samples were deoxygenated by bubbling argon for 30 min prior to measurements.

4.3. [μ-([2,2′-Bipyridyl]-5,5′-diyldi-2,1-ethynediyl)] dichlorotetrakis(tributylphosphine)diplatinum (5)

A flask charged with 9 mL of toluene and 3 mL of piperidine was purged with argon for 30 min, and then 30 mg (0.147 mmol) of 5,5′-diethynyl-2,2′-bipyridine (**4**), 214 mg (0.315 mmol) of dichlorobis(tributylphosphine) platinum and 2 mg (10.5 μmol) of copper iodide were added. The mixture was stirred at room temperature for 48 h. The solvent was removed under reduced pressure and the residue was purified by column chromatography to yield a light yellow solid (65%, 0.1424 g). ^1H NMR (300 MHz, $CDCl_3$): δ 0.93 (t, 36H), 1.49 (m, 24H), 1.56 (m, 24H), 2.02 (m, 24H), 7.57 (dd, 2H), 8.21 (d, 2H), 8.52 (d, 2H). ^{13}C NMR (75 MHz, $CDCl_3$): δ 14.0, 22.2, 24.5, 26.3, 90.5, 98.6, 120.2, 125.5, 138.3, 151.3, 152.1. ^{31}P NMR (121 MHz, $CDCl_3$): δ 8.08 (J = 2350 Hz).

4.4. p-Pt_2BPyPh

A flask charged with 5 mL of toluene and 0.5 mL of diisopropylamine was purged with argon for 30 min, and then 120 mg (0.08 mmol) of compound **5**, 33 mg (0.08 mmol) of 2,5-bisnonyloxyl-1,4-diethynylbenzene, and 1 mg (5.25 μmol) of copper iodide were added. The mixture was stirred at room temperature for 24 h. Then the mixture was poured into 50 mL of methanol and precipitates were collected. The solid was dissolved in a small amount of chloroform and filtered. The filtrate was poured into 50 mL of methanol to yield yellow precipitate. GPC: M_n = 7160, M_w = 14200. ^1H NMR (300 MHz, $CDCl_3$): 0.8–1.0 (m, 42H), 1.2–2.0 (m, 80H), 6.71 (s, 2H), 7.62 (d, 2H), 8.17(d, 2H), 8.55 (s, 2H). ^{31}P NMR (121 MHz, $CDCl_3$): δ 4.42 (J = 2352 Hz).

4.5. Pt_2BPyPh_2

It was synthesized following the same procedure described for the polymer but using two equivalents of ethynylbenzene in place of 2,5-bisnonyloxyl-1,4-diethynylbenzene. After the reaction was complete, the residue was purified by column chromatography to yield yellow solid (85%, 110 mg). ^1H NMR (300 MHz, $CDCl_3$): δ 0.93 (t, 36H), 1.46 (m, 24H), 1.51 (m, 24H), 2.13 (m, 24H), 7.10–7.28 (m, 10H), 7.60 (d, 2H), 8.18 (d, 2H), 8.56 (s, 2H). ^{13}C NMR (75 MHz, $CDCl_3$): δ 14.1, 24.1, 24.6, 26.6, 106.4, 107.6, 109.4, 115.3, 120.1, 125.1, 125.5, 128.1, 129.2, 131.0, 138.3, 151.4, 151.9. ^{31}P NMR (121 MHz, $CDCl_3$): δ 4.23 (J = 2342 Hz).

Appendix A. Supplementary data

Supplementary data associated with this article can be found, in the online version, at doi:10.1016/j.jphotochem.2009.04.013.

References

[1] A. Kraft, A.C. Grimsdale, A.B. Holmes, Angew. Chem. Int. Ed. Engl. 37 (1998) 402.
[2] J.G.C. Veinot, T.J. Marks, Acc. Chem. Res. 38 (2005) 632.
[3] C. Winder, N.S. Sariciftci, J. Mater. Chem. 14 (2004) 1077.
[4] K.M. Coakley, M.D. McGehee, Chem. Mater. 16 (2004) 4533.
[5] S. Gunes, H. Neugebauer, N.S. Sariciftci, Chem. Rev. 107 (2007) 1324.
[6] D.T. McQuade, A.E. Pullen, T.M. Swager, Chem. Rev. 100 (2000) 2537.
[7] S.W. Thomas, G.D. Joly, T.M. Swager, Chem. Rev. 107 (2007) 1339.
[8] Q. Zhou, T.M. Swager, J. Am. Chem. Soc. 117 (1995) 12593.
[9] L.H. Chen, D.W. McBranch, H.L. Wang, R. Helgeson, F. Wudl, D.G. Whitten, Proc. Natl. Acad. Sci. U.S.A. 96 (1999) 12287.
[10] K. Haskins-Glusac, M.R. Pinto, C.Y. Tan, K.S. Schanze, J. Am. Chem. Soc. 126 (2004) 14964.
[11] C.Y. Tan, E. Alas, J.G. Muller, M.R. Pinto, V.D. Kleiman, K.S. Schanze, J. Am. Chem. Soc. 126 (2004) 13685.
[12] C.Y. Tan, M.R. Pinto, M.E. Kose, I. Ghiviriga, K.S. Schanze, Adv. Mater. 16 (2004) 1208.
[13] L. Prodi, F. Bolletta, M. Montalti, N. Zaccheroni, Coord. Chem. Rev. 205 (2000) 59.
[14] Y. Zhang, C.B. Murphy, W.E. Jones, Macromolecules 35 (2002) 630.
[15] M. Kimura, T. Horai, K. Hanabusa, H. Shirai, Adv. Mater. 10 (1998) 459.
[16] B. Wang, M.R. Wasielewski, J. Am. Chem. Soc. 119 (1997) 12.
[17] Y. Wang, Z. Zhang, Y.F. Wang, L.P. Qin, W.J. Jin, Anal. Lett. 38 (2005) 601.
[18] M.L. Ho, F.M. Hwang, P.N. Chen, Y.H. Hu, Y.M. Cheng, K.S. Chen, G.H. Lee, Y. Chi, P.T. Chou, Org. Biomol. Chem. 4 (2006) 98.
[19] W.Y. Wong, Dalton Trans. (2007) 4495.
[20] T. Cardolaccia, Y.J. Li, K.S. Schanze, J. Am. Chem. Soc. 130 (2008) 2535.
[21] F.Q. Guo, K. Ogawa, Y.G. Kim, E.O. Danilov, F.N. Castellano, J.R. Reynolds, K.S. Schanze, Phys. Chem. Chem. Phys. 9 (2007) 2724.
[22] F.Q. Guo, Y.G. Kim, J.R. Reynolds, K.S. Schanze, Chem. Commun. 2006 (1887).
[23] Y. Liu, S.J. Jiang, K. Glusac, D.H. Powell, D.F. Anderson, K.S. Schanze, J. Am. Chem. Soc. 124 (2002) 12412.
[24] K. Glusac, M.E. Kose, H. Jiang, K.S. Schanze, J. Phys. Chem. B 111 (2007) 929.
[25] G.B. Kauffman, L.A. Teter, Inorganic Synthesis, vol. 7, McGraw-Hill, New York, 1963, p. 24.
[26] F.M. Romero, R. Ziessel, Tetrahedron Lett. 36 (1995) 6471.
[27] F.M. Romero, R. Ziessel, Tetrahedron Lett. 35 (1994) 9203.
[28] S. Takahashi, Y. Kuroyama, K. Sonogashira, N. Hagihara, Synthesis (1980) 627.
[29] A. Kohler, J.S. Wilson, R.H. Friend, M.K. Al-Suti, M.S. Khan, A. Gerhard, H. Bassler, J. Chem. Phys. 116 (2002) 9457.
[30] D. Beljonne, H.F. Wittmann, A. Kohler, S. Graham, M. Younus, J. Lewis, P.R. Raithby, M.S. Khan, R.H. Friend, J.L. Bredas, J. Chem. Phys. 105 (1996) 3868.
[31] E.S. Manas, L.X. Chen, Chem. Phys. Lett. 331 (2000) 299.
[32] D.K. Ryan, J.H. Weber, Anal. Chem. 54 (1982) 986.
[33] H. Linschitz, L. Pekkarinen, J. Am. Chem. Soc. 82 (1960) 2411.
[34] R.T. Farley, Ph.D. thesis, University of Florida, Gainesville, FL, 2008.
[35] A. Harriman, J. Chem. Soc. Chem. Commun. (1977) 777.